

The stability against freezing of an internal liquid-water ocean in Callisto

Javier Ruiz

Departamento de Geodinámica, Facultad de Ciencias Geológicas, and Seminar on Planetary Sciences, Universidad Complutense de Madrid, 28040 Madrid, Spain

The discovery of the induced magnetic field of Callisto—one of Jupiter’s moons—has been interpreted^{1,2} as evidence for a subsurface ocean, even though the presence of such an ocean is difficult to understand in the context of existing theoretical models^{3–5}. Tidal heating should not be significant for Callisto, and, in the absence of such heating, it is difficult to see how this internal ocean could have survived until today without freezing^{1,6}. Previous work^{3,4} indicated that an outer ice layer on the ocean would be unstable against solid-state convection, which once begun would lead to total freezing of liquid water in about 10^8 years. Here I show that when a methodology⁷ for more physically reasonable water ice viscosities (that is, stress-dependent non-newtonian viscosities, rather than the stress-independent newtonian viscosities considered previously) is adopted, the outer ice shell becomes stable against convection. This implies that a subsurface ocean could have survived up to the present, without the need for invoking antifreeze substances or other special conditions.

The moment of inertia of Callisto, as determined from measurements taken by the Galileo spacecraft, indicates that the interior of the satellite is probably partly differentiated⁸. This interpretation is in accordance with the existence of an outer water layer (frozen, liquid, or both) less than 350 km thick, overlying an interior consisting essentially (if not totally) of an ice and rock mixture, but it does not constitute as complete a differentiation as that of Ganymede⁸. It is also consistent with a depth of less than 300 km from the surface to the ocean top, as estimated from the amplitude of the induced magnetic field².

The first detailed thermal models of icy satellites (see, for example, refs 9 and 10) did not take into account the possibility of solid-state convection. They assumed heat transfer through the outermost layers by thermal conduction only (which would permit ice melting, the complete differentiation of the bodies, and the existence of thick layers of liquid water inside the satellites). Later workers^{3–5} concluded that the outer ice layers of the larger icy satellites, such as Ganymede and Callisto, are unstable against convection. The viscosity of water ice was taken as newtonian—it was described as an exponential function of temperature, but without taking into account stresses or strain rates.

An internal ocean could avoid total freezing if the ice above it was more rigid than is usually assumed, so that convective heat flow was reduced^{4,6}. Although the possibility has been mentioned that the real, non-newtonian, behaviour of water ice could have the same effect⁴, this point has not been modelled. Another way to avoid the freezing of an internal ocean is the presence of substances that lower the melting point of ice^{1,4,11}. The inclusion of ammonia could decrease the melting point to ~ 176 K (see, for example, ref. 12), and the presence of chloride salts or sulphuric acid could lower it to about 210 K (ref. 13). We note that the pioneering work of ref. 9 considered the possible role of ammonia in relation to the existence of liquid water and differentiation in Callisto. Moreover, a possible decrease of the melting point of ice owing to the presence of ammonia would also increase the viscosity of the ice shell, which in turn would reduce the convective heat flow¹⁴.

In ductile deformation, the strain rate is proportional to the applied stress: $\dot{\epsilon} \propto \sigma^n$, where n depends on the creep mechanism, and therefore on stress, temperature and grain size. Viscosity is

newtonian (independent of $\dot{\epsilon}$ and σ) if $n = 1$ (diffusion creep). On the basis of modern experimental results and theoretical considerations, it has been proposed^{15–18} that, in the low-stress (~ 0.1 MPa) conditions inside icy satellites, grain boundary sliding ($n = 1.8$ in water ice I, which is the water ice polymorph that constitutes the outer layer of Callisto^{3,4}) could be the dominant creep mechanism, at least for grain sizes less than ~ 1 mm, instead of diffusion creep as was previously thought⁵. But low stress and warm temperatures favour the growth of ice crystals, and higher grain sizes increase the relative importance of dislocation creep ($n \approx 4$ in water ice I). For that reason, it could be necessary to consider both creep mechanisms when modelling of the interior of large icy satellites¹⁹. If grain boundary sliding and dislocation creep coexist, n takes effective values between 1.8 and 4. On the other hand, diffusion creep does not seem to be a relevant deformation mechanism under planetary conditions²⁰.

In a more realistic analysis of the stability against convection of a shell of water ice I above an internal ocean in Callisto—such as I report here—non-newtonian ($n > 1$) rheological behaviour needs to be taken into account. Any substances potentially present in the water ice are not considered in my calculations, as it is not known whether they occur in amounts sufficient to produce high-degree partial melting or to alter significantly the properties of the ice. The use of water ice implies an endmember model, in which the conditions for maintaining an ocean stable against freezing are more restrictive.

The stability against convection of a layer (in this case, Callisto’s outer ice shell) can be estimated by means of the Rayleigh number defined at the layer base, Ra_{base} ; for non-newtonian viscosity, this is

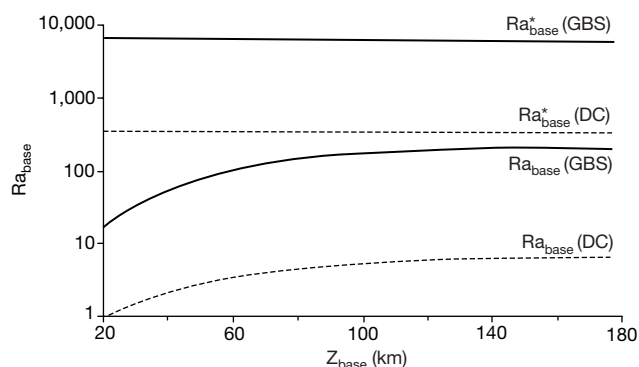


Figure 1 Stability against convection of Callisto’s outer ice shell. Ra_{base} (the Rayleigh number at the base of the outer ice shell) and Ra_{base}^* (the critical value of Ra_{base}) are shown in terms of z_{base} (the total thickness of the outer ice shell), for both grain boundary sliding (GBS) and dislocation creep (DC). Ra_{base}^* is nearly constant, and has been estimated from θ after ref. 7. For ice I, several terms involved in the calculation of Ra_{base} are functions of temperature: $\alpha = 1.56(T/250) \times 10^{-4} \text{ K}^{-1}$, and $\kappa = 1.47(250/T)^2 \times 10^{-6} \text{ m}^2 \text{ s}^{-1}$ (ref. 24), where $T = T_i$ for the convective state analysis¹⁷. The density of water ice I varies slightly with temperature and pressure, but the variations obtained from equation of state measurements for this substance are slight²⁸; therefore the adoption of a constant value does not alter the results significantly. With regard to experimentally established creep parameters: for grain boundary sliding^{15,18} $A = 9.80 \times 10^{-10} \text{ Pa}^{-n} \text{ mm}^p \text{ s}^{-1}$, $n = 1.8$, $p = 1.4$, and $Q = 49 \text{ kJ mol}^{-1}$ (Ra_{base} has been calculated for 0.1-mm grain size); and for dislocation creep²⁹ $A = 1.26 \times 10^{-19} \text{ Pa}^{-n} \text{ s}^{-1}$, $n = 4$, $p = 0$ and $Q = 61 \text{ kJ mol}^{-1}$. The creep of water ice I shows high-temperature regimes where enhanced creep rates occur. These regimes are associated with premelting effects¹⁸, or with recrystallization under stress³⁰, and have still higher values¹⁸ of Q ; they dominate at temperatures above ~ 240 – 260 K (different reports give different temperatures in this range^{18,29}). Higher values of Q reduce Ra_{base} , because—according to equations (1) and (6)— $Ra_{\text{base}} \propto A^{1/n} \exp[Q(2 - \Delta T/T_i)/nRT_i]$, and they simultaneously increase θ and Ra_{base}^* (ref. 7). Therefore, the use of the numerical values for creep parameters listed above places upper limits on Ra_{base} and lower limits on Ra_{base}^* , for both creep mechanisms—grain boundary sliding and dislocation creep.

given by⁷

$$\text{Ra}_{\text{base}} = \frac{\alpha g \rho h^{(n+2)/n} \Delta T}{\kappa^{1/n} b^{1/n}} \exp(\theta/n) \quad (1)$$

where α is the volumetric thermal expansion coefficient, g is the acceleration due to gravity (taken in general as the surface value, 1.24 m s^{-2} for Callisto), ρ is the density (930 kg m^{-3} for water ice I), h is the effective layer thickness, $\Delta T (= T_{\text{base}} - T_s)$ is the temperature difference between the base and the surface of the layer, κ is the thermal diffusion coefficient, b is a parameter that depends on creep mechanism and temperature, and n is a constant that depends on creep mechanism. $\theta (= Q\Delta T/RT_i^2)$ is the Frank–Kamenetskii parameter (which is related to the viscosity contrast through the layer caused by temperature differences), where Q is the activation enthalpy of creep deformation (which, because of experimental uncertainty, can be taken as the activation energy), R is the gas constant, and T_i is the adiabatic temperature (approximately constant) in the case of convection. If, for a definite value of θ , Ra_{base} does not reach a certain critical value $\text{Ra}_{\text{base}}^*$ (estimated after ref. 7), a layer in thermal conductive equilibrium is stable against convection.

To solve equation (1), it is necessary to make a reasonable estimate of T_{base} , T_i and h . Before the onset of convection, heat is transmitted into Callisto's outer shell only by conduction. As there is no tidal heating in Callisto^{1,3,21}, I considered an outer shell in conductive thermal equilibrium, and heated from below by radioactive disintegration in the interior rocky fraction underneath the ocean. Under these conditions, the variation of temperature with depth can be described through Fourier's law,

$$dT = (F_z/k) dz \quad (2)$$

where F_z is the vertical heat flow at a depth z from surface, and k is the thermal conductivity. For ice I, k is a function of temperature ($k = k_0/T$, where k_0 is a constant with a value of 567 W m^{-1} (ref. 22)); also, in a spherical layer in energetic equilibrium heated from below, $F_z = r^2 F / (r - z)^2$, where r is the body radius, and F is the heat flow at the surface. If both expressions for k and F_z are substituted in equation (2), and the equation is then integrated from the surface to z_{base} (z_{base} is the total thickness of the outer ice shell), an equation for temperature at the base of the outer ice shell is obtained:

$$T_{\text{base}} = T_s \exp \left[\frac{r F z_{\text{base}}}{k_0 (r - z_{\text{base}})} \right] \quad (3)$$

where T_s is taken as 130 K (ref. 23). At the same time, if the Clapeyron slope for melting ice is taken as $-0.1063 \text{ K MPa}^{-1}$ (ref. 24), T_{base} (in K) can be approximated as

$$T_{\text{base}} = 273.16 - 0.1063 P_{\text{base}} \quad (4)$$

where P_{base} (in MPa) is the pressure at the outer shell base, given by integration from the surface to z_{base} of $\rho G M_z / (r - z)^2 dz$, where in turn G is the gravitational constant, and M_z is the mass of a sphere with radius $(r - z)$ (the total mass of Callisto is $2.5 \times 10^{23} \text{ kg}$). If equations (3) and (4) are resolved simultaneously, z_{base} and T_{base} are obtained. Because thermal conductivity is a function of temperature, h is not the real layer thickness z_{base} before the onset of convection, but an effective thickness¹⁷, which is defined for a situation of conductive thermal equilibrium with the constant thermal conductivity corresponding to T_i ; the convective analysis followed here assumes a cartesian geometry⁷, and for that reason $h = k_0 \Delta T / FT_i$.

Convection on icy satellites would involve a stagnant-lid regime²⁶, in which the upper part of an outer shell does not participate in the convective movement. The temperature contrast across the lower boundary layer of the convecting region, $T_{\text{base}} - T_i$, can be taken as the rheological temperature scale²⁷, $\sim \Delta T / \theta$, and for that reason T_i can be estimated approximately from:

$$T_{\text{base}} - T_i \approx RT_i^2 / Q \quad (5)$$

The effective viscosity for a non-newtonian rheology can be described by $\eta = (d^p/A)\sigma_{\text{II}}^{1-n} \exp(Q/RT)$, where d is the grain size, p and A are experimentally established constants, and σ_{II} is the second invariant of the deviatoric stress tensor. In some work on solid-state convection^{7,27}, the use of the Frank–Kamenetskii approximation ($\eta = b\sigma_{\text{II}}^{1-n} \exp(-QT/RT_i^2)$) as the value of the effective viscosity has been proposed. If the condition is imposed that both expressions give the same η value in $T = T_i$, b can be estimated in T_i from:

$$b = (d^p/A) \exp(2Q/RT_i) \quad (6)$$

I performed the analysis for both grain boundary sliding and dislocation creep, according to the discussion above. Grain boundary sliding is a grain-size-sensitive creep mechanism, in which smaller grain sizes diminish the b value, thus conversely increasing Ra_{base} . For that reason, I have taken a grain size of 0.1 mm : the existence of smaller grain sizes does not seem a realistic possibility for the interiors of large icy satellites¹⁷, and therefore this value implies a reasonable upper limit in the estimation of Ra_{base} for grain boundary sliding. On the other hand, dislocation creep is independent of grain size, and for that reason $p = 0$.

The results are given in Fig. 1; they are shown as Ra_{base} in terms of z_{base} and compared with the corresponding $\text{Ra}_{\text{base}}^*$ values, for both grain boundary sliding and dislocation creep. z_{base} increases gradually with time as F diminishes because of power loss of the internal heat sources. If the present surface heat flow is taken as $\sim 3.6 \text{ mW m}^{-2}$, then today $z_{\text{base}} \approx 105 \text{ km}$. The value of $\sim 3.6 \text{ mW m}^{-2}$ is the mean value of the heat flow interval estimated as a function of the degree of differentiation and of the rock models for the rocky fraction of Callisto²³: it varies from 3.3 mW m^{-2} (Callisto undifferentiated) to 3.9 mW m^{-2} (Callisto completely differentiated). On the other hand, $F \approx 2 \text{ mW m}^{-2}$ and $z_{\text{base}} = 176.5 \text{ km}$ corresponds to the minimal melting point as a function of the pressure of ice (at 251.1 K and 207 MPa , ref. 24).

The data in Fig. 1 show that Callisto's conductive ice shell is at present stable against solid-state convection—because the values of Ra_{base} are always much lower than those of $\text{Ra}_{\text{base}}^*$, for both grain boundary sliding and dislocation creep. These results are important, because they imply that a conductive outer shell would also have been stable against convection in the past.

This calculated stability of an internal ocean and a non-convecting ice shell could be consistent with the observed geology of Callisto. It could be argued that the heavily cratered surface of Callisto, and the lack of clear geological modifications originating from under the surface, are evidence against the existence of a subsurface ocean¹; but if the icy shell is stable and convectively inactive, and if the cold, brittle lithosphere is very thick, geological inactivity of the shell (compared to those of the tidally heated^{4,21} jovian satellites Europa and possibly Ganymede) can be understood.

Finally, according to these results for Callisto, a consequence of the non-newtonian nature of water ice I could be that it is more difficult than previously thought to obtain convection in the external layers of icy satellites. If this is correct, the existence of oceans under ice in great icy satellites could be a common phenomenon. \square

1. Khurana, K. K. *et al.* Induced magnetic fields as evidence for subsurface oceans in Europa and Callisto. *Nature* **395**, 777–780 (1998).
2. Zimmer, C., Khurana, K. K. & Kivelson, M. G. Subsurface oceans on Europa and Callisto: Constraints from Galileo magnetometer observations. *Icarus* **147**, 329–347 (2000).
3. Reynolds, R. T. & Cassen, P. M. On the internal structure of the major satellites of the outer planets. *Geophys. Res. Lett.* **6**, 121–124 (1979).
4. Cassen, P. M., Peale, S. J. & Reynolds, R. T. in *Satellites of Jupiter* (ed. Morrison, D.) 93–128 (Univ. Arizona Press, Tucson, 1982).
5. Schubert, G., Spohn, T. & Reynolds, R. T. in *Satellites* (eds Burns, J. A. & Matthews, M. S.) 224–292 (Univ. Arizona Press, Tucson, 1986).
6. Showman, A. P. & Malhotra, R. The Galilean satellites. *Science* **286**, 77–84 (1999).
7. Solomatov, V. S. Scaling of temperature- and stress-dependent viscosity convection. *Phys. Fluids* **7**, 266–274 (1995).
8. Anderson, J. D. *et al.* Distribution of rock, metals, and ices in Callisto. *Science* **280**, 1573–1576 (1998).

9. Lewis, J. S. Satellites of the outer planets: thermal models. *Science* **172**, 1127–1128 (1971).
10. Consolmagno, G. J. & Lewis, J. S. The evolution of icy satellite interiors and surfaces. *Icarus* **34**, 280–293 (1978).
11. Stevenson, D. J. An ocean within Callisto? *Eos* **79**, F535 (1998).
12. Kargel, J. S. Ammonia-water volcanism on icy satellites: Phase relations at 1 atmosphere. *Icarus* **100**, 556–574 (1992).
13. Kargel, J. S. *et al.* Europa's crust and ocean: origin, composition, and the prospects for life. *Icarus* **148**, 226–265 (2000).
14. Sotin, C., Grasset, O. & Beauchesne, S. in *Solar System Ices* (eds Schmitt, B., De Bergh, C. & Festou, M.) 79–96 (Kluwer Academic, Dordrecht, 1998).
15. Goldsby, D. L. & Kohlstedt, D. L. Grain boundary sliding in fine-grained ice I. *Scripta Mater.* **37**, 1399–1406 (1997).
16. Pappalardo, R. T. *et al.* Geological evidence for solid-state convection in Europa's ice shell. *Nature* **391**, 365–368 (1998).
17. McKinnon, W. B. Convective instability in Europa's floating ice shell. *Geophys. Res. Lett.* **26**, 951–954 (1999).
18. Goldsby, D. L. & Kohlstedt, D. L. Superplastic deformation of ice: Experimental observations. *J. Geophys. Res.* (in the press).
19. Durham, W. B., Kirby, S. H. & Stern, L. A. The rheology of ice I at low stress and elevated confining pressure. *J. Geophys. Res.* (in the press).
20. Goldsby, D. L. & Kohlstedt, D. L. Flow of ice I by dislocation, grain boundary sliding, and diffusion processes. *Lunar Planet. Sci. XXVIII*, 429–430 (1997).
21. Showman, A. P. & Malhotra, R. Tidal evolution into Laplace resonance and the resurfacing of Ganymede. *Icarus* **127**, 93–111 (1997).
22. Klinger, J. Influence of a phase transition of the ice on the heat and mass balance of comets. *Science* **209**, 271–272 (1980).
23. Mueller, S. & McKinnon, W. B. Three-layered models of Ganymede and Callisto: Compositions, structures, and aspects of evolution. *Icarus* **76**, 437–464 (1988).
24. Kirk, R. L. & Stevenson, D. J. Thermal evolution of a differentiated Ganymede and implications for surface features. *Icarus* **69**, 91–134 (1987).
25. Davies, M. E. *et al.* The control networks of the Galilean satellites and implications for global shape. *Icarus* **135**, 372–376 (1998).
26. McKinnon, W. B. in *Solar System Ices* (eds Schmitt, B., De Bergh, C. & Festou, M.) 525–550 (Kluwer Academic, Dordrecht, 1998).
27. Solomatov, V. S. & Moresi, L.-N. Stagnant lid convection on Venus. *J. Geophys. Res.* **101**, 4737–4753 (1996).
28. Lupo, M. J. & Lewis, J. S. Mass-radius relationships in icy satellites. *Icarus* **40**, 157–170 (1978).
29. Durham, W. B., Kirby, S. H. & Stern, L. A. Creep of water ices at planetary conditions: A compilation. *J. Geophys. Res.* **102**, 16293–16302 (1997).
30. Kamb, B. in *Flow and Fracture of Rocks* (eds Heard, H. C., Borg, I. Y., Carter, N. L. & Raleigh, C. B.) 211–241 (AGU Geophys. Monogr. Ser. 16, American Geophysical Union, Washington DC, 1972).

Acknowledgements

I thank F. Anguita, O. Prieto, J. Ruiz, R. Tejero and A. Torices for suggestions, K. Bennett and J. Kargel for comments on the manuscript, and W. Durham and D. Goldsby for preprints of work in press.

Correspondence and requests for materials should be addressed to the author (e-mail: jaruiz@eucmax.sim.ucm.es).

Evidence for recent climate change on Mars from the identification of youthful near-surface ground ice

John F. Mustard, Christopher D. Cooper & Moses K. Rifkin

Department of Geological Sciences, Brown University, Providence, Rhode Island 02912, USA

Ground ice in the crust and soil may be one of the largest reservoirs of water on Mars^{1–3}. Near-surface ground ice is predicted to be stable at latitudes higher than 40° (ref. 4), where a number of geomorphologic features indicative of viscous creep and hence ground ice have been observed⁵. Mid-latitude soils have also been implicated as a water-ice reservoir⁶, the capacity of which is predicted to vary on a 100,000-year timescale owing to orbitally driven variations in climate⁷. It is uncertain, however, whether near-surface ground ice currently exists at these latitudes, and how it is changing with time. Here we report observational evidence for a mid-latitude reservoir of near-surface water ice occupying the pore space of soils. The thickness of the ice-occupied soil reservoir

(1–10 m) and its distribution in the 30° to 60° latitude bands indicate a reservoir of $(1.5–6.0) \times 10^4 \text{ km}^3$, equivalent to a global layer of water 10–40 cm thick. We infer that the reservoir was created during the last phase of high orbital obliquity less than 100,000 years ago, and is now being diminished.

Using high-resolution images from the Mars Orbiter Camera (MOC) on the Mars Global Surveyor (MGS) spacecraft^{8,9}, we have identified and mapped on a global scale a unique, young terrain on Mars that exhibits a morphology consistent with a material that has been cemented and then partially dissected (cut into hills and valleys) or disaggregated. The terrain (Fig. 1) is recognized on the basis of the following criteria: (1) a smooth, intact surface is present; (2) the smooth material is broken up or dissected somewhere in the

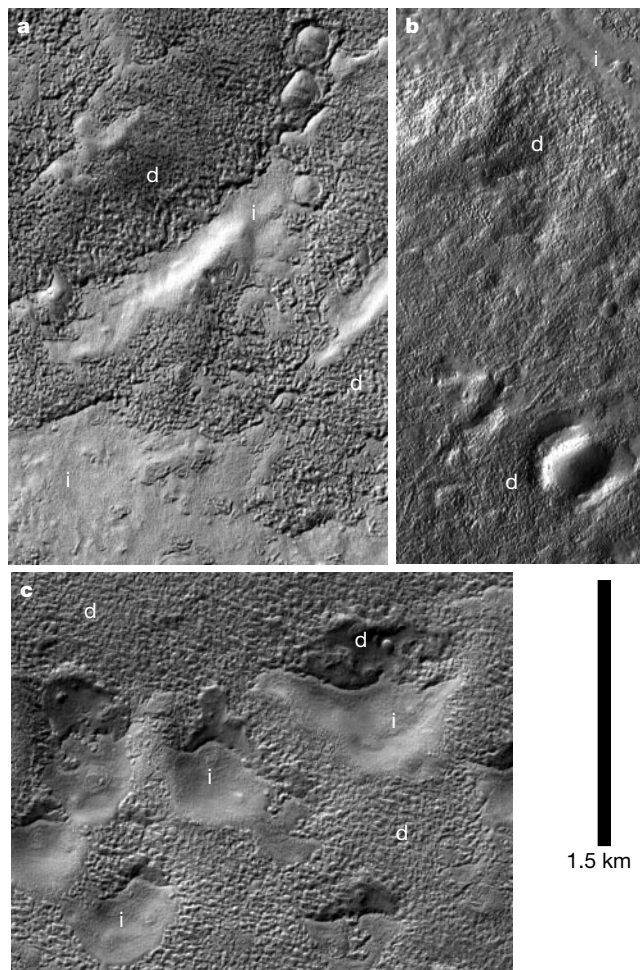


Figure 1 Examples of terrain interpreted to contain near-surface ground ice. The scale is the same for all images and in each image 'i' indicates intact terrain and 'd' indicates dissected (eroded) terrain. Illumination is from below and the nearest pole is towards the top of each image. **a**, A large expanse of intact terrain with incipient dissection into numerous steep-walled pits and troughs a few metres in size. The layer thickness is estimated to be 10 m. **b**, The amount of dissection is greater and clearly demonstrates the lack of preferred orientation and pattern in the dissected terrain. Here the layer thickness is estimated to be 2 m. **c**, The dissected layer in this region, estimated to be 5 m thick, is completely removed in places, revealing the substrate beneath. In these three examples, the density of pits ranges from sparse to abundant. The pitted surface grades into a knobby terrain which further grades into a rough surface. In areas of complete degradation a relict surface is revealed. The gradations between the smooth, pitted, knobby and rough surfaces imply a process where the smooth unit disaggregates and is removed to reveal a pre-existing surface. **a**, Image M0400837 (43.40° N, 240.21° W), $i = 55.31^\circ$; **b**, image SP253404 (34.35° N, 356.00° W), $i = 74.67^\circ$; **c**, image FHA01450 (43.71° S, 239.61° W), $i = 75.49^\circ$.